ISSN 0010-5082, Combustion, Explosion, and Shock Waves, 2017, Vol. 53, No. 3, pp. 319–328. © Pleiades Publishing, Ltd., 2017.
Original Russian Text © P. Ma, J.-Ch. Jiang, Sh.-G. Zhu.

Synthesis, XRD and DFT Studies of a Novel Cocrystal Energetic Perchlorate Amine Salt: Methylamine Triethylenediamine Triperchlorate

P. Ma[a], J.-Ch. Jiang[a], and Sh.-G. Zhu[b]

UDC 536.45

Published in *Fizika Goreniya i Vzryva*, Vol. 53, No. 3, pp. 82–92, May–June, 2017.
Original article submitted April 5, 2016; revision submitted August 18, 2016.

Abstract: This paper reports the synthesis, experimental and theoretical studies of a novel inorganic-organic cocrystal energetic material: methylamine triethylenediamine triperchlorate (MT). MT is synthesized by a rapid "one-pot" method. The performance test of MT shows that it is more powerful and has lower sensitivity in comparison to the benchmark energetic material, i.e., 2,4,6-trinitrotoluen (TNT). The molecular and crystal structures of MT are determined by means of x-ray diffraction (XRD). The compound crystallizes in a monoclinic system (space group Pn) with cell dimensions $a = 8.975(18)$, $b = 17.836(4)$, and $c = 10.455(2)$ Å. The band structure and the density of states are calculated by an abbreviated form of the CASTEP code. The first principle tight-binding method within the general gradient approximation is used to study the electronic band structure, density of states, and Fermi energy. The results indicate that the main mechanism of cocrystallization originates from the Cl—O $\cdots$ H hydrogen bonding between —ClO_4 and —NH_2.

Keywords: cocrystal energetic material, crystal structure, performance, DFT calculation.

DOI: 10.1134/S0010508217030091

INTRODUCTION

Energetic materials are a class of compounds with much chemical energy stored in their structure, which are widely used both in military and civil engineering [1–4]. Now more and more scientists are trying to synthesize new kinds of energetic materials with properties of higher energy and lower sensitivity [5, 6]. However, it is not easy to find such materials that possess both a high detonation speed and low sensitivity [7–9]. The cocrystallization technology introduces a new way to obtain high-energy-density materials with excellent performance [10–12].

Cocrystallization is widely used in pharmaceutical chemical areas because it can combine two or more components together by using weak interactions without destroying the chemical structure [13, 14]. Therefore, the cocrystallization technology can be used in the area of energetic materials to modify the performance, such as the energy and sensitivity [15, 16]. By using this method, outstanding contributions in the field of energetic materials were made in [17–24]. Various cocrystal energetic materials with excellent performance, such as higher density, better thermal stability, etc., were reported. Until now, nearly all the reported cocrystal energetic materials (CoEMs) have been organic compounds, such as CL-20/HMX [20] and CL-20/TNT [25], because of the easy formation of hydrogen bonds. Most of the CoEMs can be only prepared in a laboratory grade, which limits their wide application because of the low yield. Meanwhile, the synthesis of inorganic compounds is fast and provides a high yield. Our previous work shows that inorganic cocrystal energetic salts con-

[a] Jiangsu Key Laboratory of Hazardous Chemicals Safety and Control, College of Safety Science and Engineering, Nanjing Tech University, Nanjing, 210009 China; mapengcn@hotmail.com.
[b] School of Chemical Engineering, Nanjing University of Science and Technology, Nanjing, 210094 China.

sisting of amine and perchlorate are characterized by low sensitivity and high energy [26, 27]. Also, they are easy to be prepared from raw materials that are widely used and are not expensive. At the same time, plenty of hydrogen bonds in amine perchlorate compounds indicate the possibility for the formation of cocrystals.

In the present work, a new kind of an inorganic-organic cocrystal energetic material, namely, methylamine triethylenediamine triperchlorate (MT) was synthesized. The synthesis method was described. The crystal structure was analyzed. A density functional theory calculation was employed to find out the relationship between the hydrostatic pressure and crystal structure.

1. EXPERIMENTAL TECHNIQUE

The title compound (MT) is an energetic material that tends to explode under certain conditions. Therefore, appropriate safety precautions are required. CoEM generating can be divided into two steps: the first step is to obtain ligands (such as Cl-20 and TNT), and the next step is cocrystallization. In this paper, we introduce a new "one-pot" synthesis method, which can be considered as a simplified two-stage method: the raw materials are charged into one reactor and a cocrystal is formed when the reaction is finalized.

The sample used in this work was prepared by the following method: 10 ml of methylamine and 0.03 g of triethylenediamine were charged into a glass reactor containing 50 ml of distilled water. The charged substances were kept under mechanical stirring. Then 36 g of perchlorate acid were dropwise added to the glass reactor, which resulted in a vigorous exothermic reaction leading to an increase in the temperature of the content. The solution turned from turbid to clear, and the temperature of the solution rapidly increased. The temperature should be controlled below 70°C; otherwise, the solution would turn to yellow and the quality of the product would be deteriorated. The solution obtained was stirred for 30 min. Then, it was naturally cooled to room temperature and allowed to stand for 1 h until a white precipitate was formed. After that, the content of the reaction flask was continuously stirred at room temperature until white crystals of MT were obtained. The crystals were washed with alcohol (50 ml) three times and dried at 60°C. The mother liquor was collected for recycling so the theoretical yield was 100% [25]. The elemental analysis of MT was performed by using the Vario MICRO cube analyzer (Germany). The theoretical elemental composition was 18.90% C, 4.50% H, 23.96% Cl, 9.43% N, and 43.19% O; the experimental results were 18.89% C, 4.50% H, 23.97% Cl, 9.42% N, and 43.20% O.

1.1. X-ray Crystallography

A TM compound with the edges of 0.30 × 0.20 × 0.20 mm was studied at 293 (±2) K by using a CAD4/PC four-circle diffractometer with graphite-monochromatized radiation MoK_α ($\lambda = 0.71074$ Å).

The data were obtained in the $\omega/2\theta$ scan mode, with three standard reflections measured every 120 min. Data reduction was carried out using the XCAD-4 program. An absorption correction based on the ψ-scan method was applied. The structure was solved by direct methods and refined by the full-matrix least-squares technique on F2 with anisotropic thermal parameters for all non-hydrogen atoms using the SHELXS97 program [28]. All hydrogen atoms were located from different Fourier maps and refined isotropically. Detailed information on crystallographic data collection and structure refinement is provided in Table 1.

1.2. Structure Description

The asymmetric unit of MT shown in Fig. 1 consist of one methylamine cation, two triethylenediamine cations, and six perchlorate anions. The organic cation and the inorganic anion are held together by hydrogen bonds N—H $\cdots$ O (see Fig. 1 and Table 2). Hydrogen bonds can form intermolecular and intramolecular interactions, so it can be seen from Fig. 1 that a zigzag chain structure is generated between the crystals, i.e., MT is a kind of a supramolecular structure. An intermolecular hydrogen bond is formed between the methylamine cation and the perchlorate anion and also between the triethylenediamine cation and the perchlorate anion. In particular, hydrogen from methylamine can form three different hydrogen bonds, which are called trigeminal-type hydrogen bonds (Fig. 2). This typical kind of inter- and intramolecular hydrogen bonds can stabilize the crystal lattice to a large extent.

The calculations are performed using the CASTEP code implemented in the Materials Studio 4.4 environment [29]. The code is an ab initio quantum mechanics code based on the density functional theory (DFT). Geometry optimization was carried out by using the Broyden–Fletcher–Goldfrab–Shanno (BFGS) method [30]. Our previous work showed that standard DFT methods, such as the latent Dirichlet allocation (LDA) and generalized gradient approximation (GGA), are suitable for this kind of cocrystals. In order to test the accuracy of the LDA and GGA methods, we compared the calculated lattice parameters and cell volume with experimental data (Table 3). As compared to experimental data, the volume obtained by the LDA method is lower by 9%, while that predicted by the GGA method is larger by 6%. Concerning the

Table 1. Crystal parameters and structure refinement for the MT compound

Empirical formula	$C_{14}H_{40}Cl_6N_6O_{24}$
Molecular weight	889.22
Temperature, K	293(2)
Wavelength, Å	0.71073
Crystal structure	Monoclinic
Space group	Pn
a, Å	8.9750(18)
b, Å	17.836(4)
c, Å	10.455(2)
α, deg	90.00
β, deg	91.30(3)
γ, deg	90.00
Volume, Å^3	1673.2(6)
Z	2
Crystal size, mm^3	0.30 × 0.20 × 0.20
Density (calculated), mg/m^3	1.865
$F(000)$	920
Absorption coefficient	0.616
θ-range for data collection, deg	1.14–25.36
Goodness-of-fit on F2	1.007

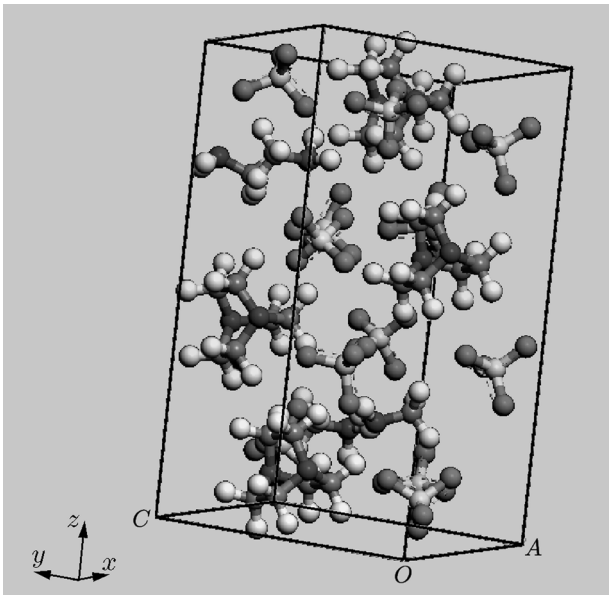

Fig. 1. Molecular unit of MT

Table 2. Intermolecular interaction distances and angles of MT

Donor—H···Acceptor	D—H, Å	H···A, Å	D···A, Å	D—H···A, deg
N(1)—H(1A)···O(3)	1.051	1.776	2.622	134.4
N(1)—H(1A)···O(8)	1.051	1.941	2.597	117.3
N(1)—H(1A)···O(18)	1.051	2.258	2.809	110.8
N(2)—H(2A)···O(2)	1.049	1.99	2.613	114.9
N(2)—H(2A)···O(7)	1.049	1.95	2.64	120.3
N(2)—H(2A)···O(20)	1.049	2.127	2.767	117

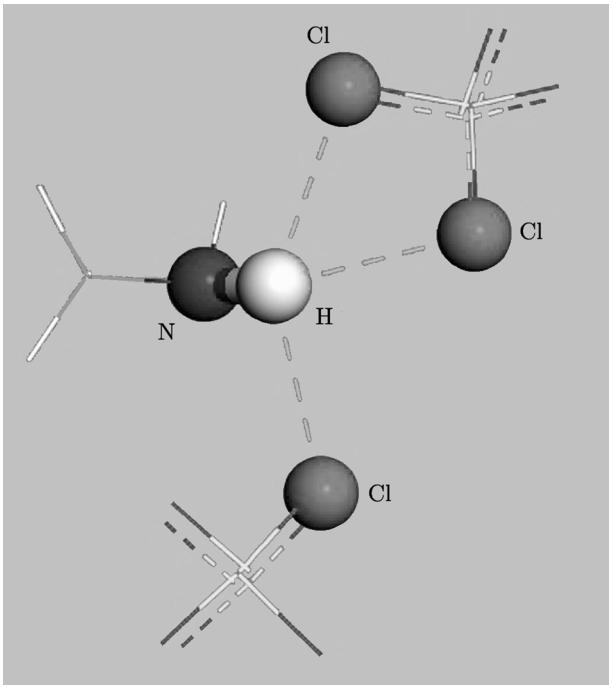

Fig. 2. Trigeminal hydrogen bond.

lattice parameters, the GGA method is much closer to experimental data. As a whole, the standard DFT method GGA reproduces well the ground state structure and can be employed to calculate other properties. On-the-fly (OTF) pseudopotentials generated by using the CASTEP software package were used, along with a plane-wave cutoff energy of 650 eV, which ensured convergence of both lattice parameters and total energies (to less than 5 meV per unit cell). The Brillouin zone sampling was performed by using the Monkhost–Pack scheme with a 2 × 3 × 1 K-point grid. The starting atomic coordinates were taken from the final x-ray refinement cycle. The structures were relaxed (by the BFGS method) to allow both atomic coordinates and unit cell vectors to be optimized simultaneously,

Table 3. Comparison of the calculated parameters of the MT crystal lattice

Method	a, Å	b, Å	c, Å	V, Å^3
LDA	8.346	15.964	11.386	1519.32
GGA	9.025	17.772	11.037	1770.15
Experiment	8.975	17.836	10.455	1673.19

Table 4. Measured velocities of detonation for MT, TNT, and HMX

Substance	ρ, g/cm^3	D, m/s
MT	1.204	6356
	1.537	7102
TNT	1.620	6900
HMX	1.890	9110

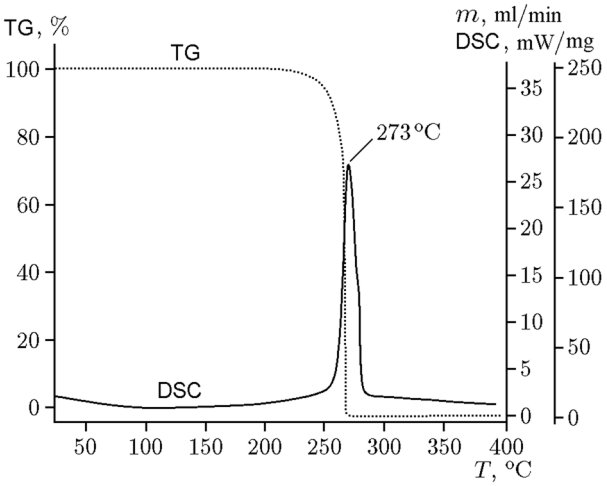

Fig. 3. DSC and TG curves for MT.

while constraining space group symmetry [the convergence criteria were the maximum change in the system energy of $2 \cdot 10^{-5}$ eV, the maximum root-mean-square (RMS) force of 0.025 eV/Å, the maximum RMS stress of 0.01 GPa, and the maximum RMS displacement of 0.002 Å].

2. RESULTS AND DISCUSSION

2.1. Performance Test

Sensitivity is a key property for energetic materials because it is closely linked with the safety of handling and applying. The impact sensitivity was measured for the MT cocrystal by using the Kast drop hammer apparatus with a 10 kg drop hammer. The components of MT, PETN, and TNT were also tested. Each material was tested by using 30 ± 0.05 mg samples. The impact sensitivity of MT was found to be $H_{50} = 8.75$ cm, which means a 50% probability of detonation at this height. The impact sensitivity was $H_{50} = 4.43$ cm for PETN and $H_{50} = 15.81$ cm for TNT. It is seen that MT is a much safer material than PETN, but more sensitive to an impact than TNT. Therefore, MT can be used as both primary and secondary explosives.

The detonation velocities (D) of MT, HMX, and TNT were tested by a ZBS-10A100MHz intelligent ten segments detonation velocity measuring instrument at room temperature (Table 4). The detonation velocity is a critical property to evaluate the performance of energetic materials. The density exerts an important effect on the detonation velocity: the higher the density of energetic materials, the higher the detonation velocity. MT samples (20 ± 0.05 g) for the detonation velocity tests were shaped as cylinders with diameters of 10.0 ± 0.1 mm. The lowest detonation velocity (6356 m/s) was measured for low-density MT cocrystals ($\rho = 1.204$ g/cm^3). In MT cocrystals with a higher density ($\rho = 1.537$ g/cm^3), the detonation velocity (7102 m/s) was much higher than that for TNT (6900 m/s), but still slightly lower than that for HMX (9110 m/s). This may be explained by the lower density of the MT cocrystal as compared to HMX.

2.2. Thermal Analysis

The differential scanning calorimetry (DSC) and thermogravimetry (TG) methods were employed to study the thermal decomposition of MT (Fig. 4). The DSC trace of MT shows a strong exothermic peak at 273°C, much higher than that of TNT (210°C) and CL-20 (245–249°C) [31]. The TG curve of MT shows only one weight loss step, appearing in the temperature range of 250–280°C, which is mainly attributed to intense thermal decomposition of MT.

2.3. Band Structure

The band structure plays an important role in optoelectronic materials. The exchange correlation potential was defined by using the GGA method based on geometry optimization, and the electron–ion interaction was described by an ultrasoft potential generated. The calculated band structure and density of states are shown in Figs. 4 and 5, respectively.

Several studies [32–36] reported that the electronic structure of energetic compounds produces a significant effect on their structures and properties. Zhu and

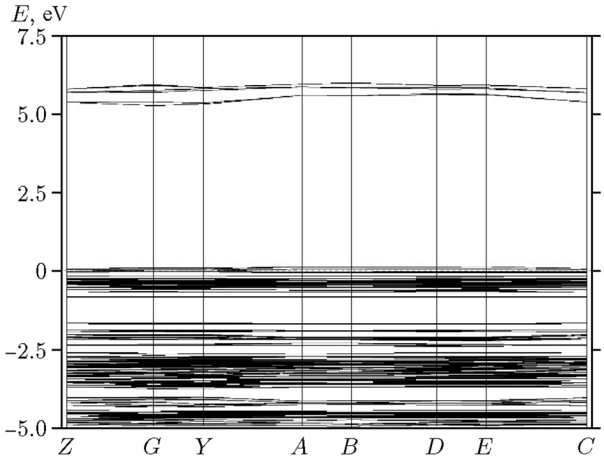

Fig. 4. Energy band structure for MT.

Xiao [37] reported the relationship between the band gap and sensitivity: the smaller the band gap, the easier it is to transfer an electron from the valence bands to the conduction bands; consequently, an external stimulus can more easily decompose the energetic material, leading to an explosion. The band gap of MT is 1.6 eV between the valence and conduction bands, i.e., MT is an insulator and has a low sensitivity. It is seen from Fig. 4 that the band structure is simple and appears to differ from the SY cocrystal from our previous work [26] only in the energy band width. The curves of the total density of states shown in Fig. 5 have five main peaks: P1, P2, and P3 in the valence bands, and also P4 and P5 forming the conduction bands. The curves of the partial density of states for MT reveal that the C-*sp*, Cl-*sp*, N-*sp*, and O-*sp* orbitals overlap over the energy ranges from −30 to 10 eV, which is evidently indicative of covalent interactions between them resulting from strong hybridization. It is seen from Fig. 5 that the lowest-lying bands arise from the 2*s*- and 2*p* states of Cl and N, while the bands in the valence region just below the Fermi energy are predominantly due to the 2*p* states of C, Cl, N, and O, which is different from the results for the SY cocrystal [27]. It is found that the top of the valence bands has large dispersion, whereas the bottom of the conduction bands has rather small dispersion, which is similar to SY [26]. The lowest energy of the conduction bands (1.62 eV) and the highest energy of the valence bands (0 eV) are both localized at the point *G*. The valence bands between −20.0 and −15.0 eV are created by the 2*p* states of N, O, and Cl, mixing with low 2*s* states of C and Cl. The valence bands between −15.0 and 0 eV are mostly created by the 2*p* states of N, O and, Cl. The conduction bands between 0 and 10.0 eV are mostly formed due to the

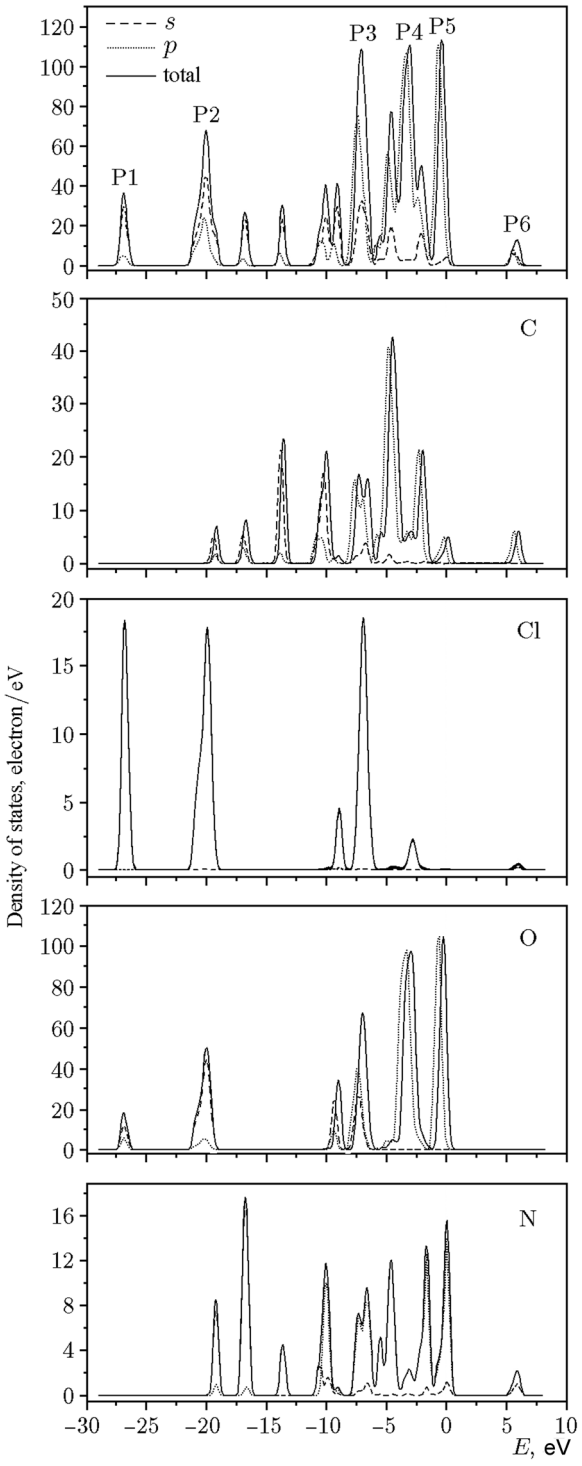

Fig. 5. Total and partial density of states in MT.

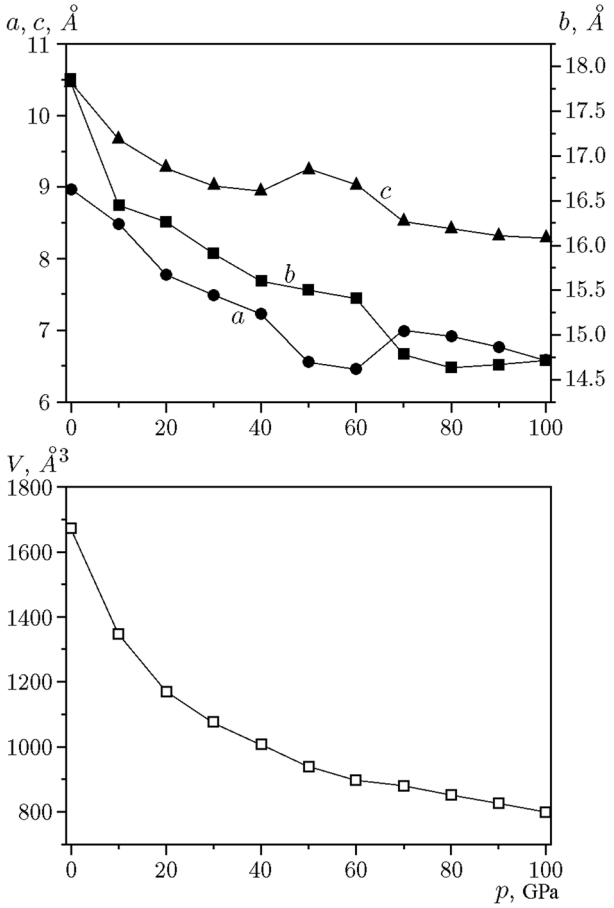

Fig. 6. Lattice parameters under high pressure.

contribution from the O-2p- and C-2p states hybridized with a small amount of the N-2s, N-2p, Cl-2s, and Cl-2p states.

2.4. Structure under High Pressure

When an energetic material explodes, the pressure increases up to 30 GPa. Thus, it is necessary to investigate the band gap of MT at different pressures. The relaxed lattice constants of MT at different hydrostatic pressures (0–100 GPa) are shown in Fig. 6. It can be seen that the lattice parameters (a, b, and c) and the volume V decrease as the pressure p increases up to 40 GPa. It is worth noting that b and c increase abnormally in the pressure range p = 40–80 GPa. Moreover, the value of V slightly increases at p = 70 GPa. It can be deduced that structural transformations may happen in these ranges of pressure. Obviously, the lattice parameters decrease sharply at $p \leqslant 40$ GPa, i.e., the unit cell can be easily compressed in this region. In the pressure range p = 0–40 GPa, the compressions of a, b, c, and V are 19.45, 12.54, 14.50, and 39.86%, respec-

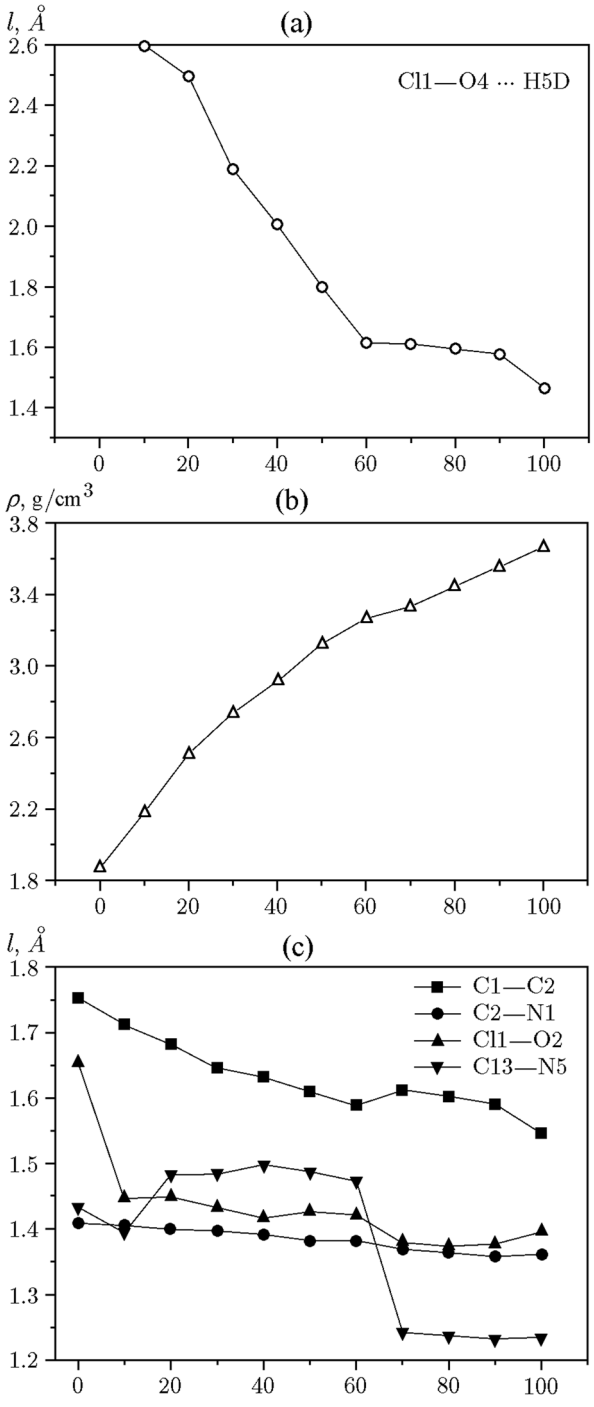

Fig. 7. Hydrogen bond length and density of the optimized unit cell versus pressure.

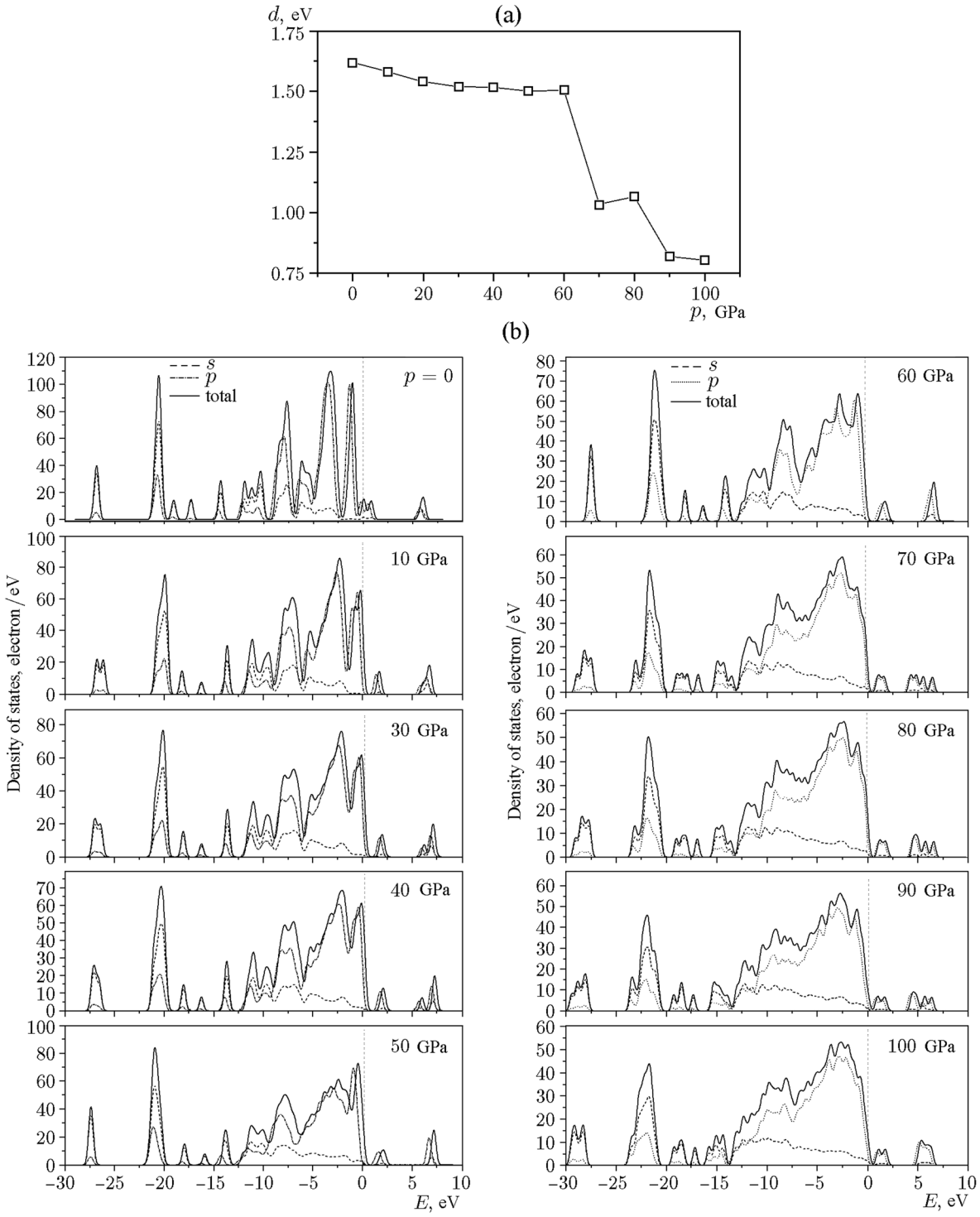

Fig. 8. Band gap (a) and density of states in the MT cocrystal (b) for different pressures.

tively, which are much greater than 2.1, 5.09, 10.53, and 14.80% in the pressure range $p = 50$–100 GPa. In the low-pressure area, the distance between the molecules is large; hence, the intermolecular repulsion is rather low. Therefore, the crystal is easily compressed as compared to the chemical bond. In the high-pressure range, however, the intermolecular repulsion is much more intense, and the crystal is difficult to be compressed. Obviously,

the compressibilities along three directions are different, which indicates that the compressibility of the crystal is anisotropic.

As the pressure increases, the distance between the atoms becomes closer, which may influence the length of the hydrogen bonds in MT. The length of the hydrogen bond (Cl1—O4 ⋯ H5D) as a function of pressure is shown in Fig. 7a. It is seen that the length of the hydrogen bond decreases as the pressure increases. This decrease is abrupt up to $p = 60$ GPa and smooth at $p =$ 60–100 GPa. Thus, the strength of the hydrogen bonds increases due to a decrease in the bond length. Hence, the crystal becomes more stable. However, an increase in pressure leads to an increase in density (Fig. 7b). A higher density means a more intense energy release when blasting; therefore, the pressure-induced density enlargement would enhance the detonation performance of MT.

As discussed above, both the unit cell and the cocrystal geometry are affected by hydrostatic pressure. Therefore, the bond length may also be influenced by external pressure. Figure 7c shows the change in the length of selected bonds (C1—C2, C2—N1, Cl1—O2, and C13—N5) at different pressures. Some bonds, such as C1—C2 and Cl1—O2, shorten gradually and monotonically, while the C13—N5 bond length increases at $p = 20$ GPa and decreases drastically at $p = 70$ GPa. The C2—N1 bond changes only slightly, which indicates that the group of triethylenediamine cannot be compressed. The change in the bond length shows that the Cl1—O2 bond can be compressed easier than other bonds in the low-pressure zone (0–10 GPa). In the pressure range $p = 20$–60 GPa, all bonds shorten gradually, except for C13—N5, which lengthen a bit. In the high-pressure area, the C13—N5 bond suddenly shortens from 1.47 to 1.23 Å. This indicates that methylamine is more likely to be compressed.

2.5. Electronic Structure

The band gaps d of MT were also calculated as functions of pressure (Fig. 8a). As a whole, the band gap decreases with an increase in pressure. In the range $p = 0$–60 GPa, the band gap gradually decreases from 1.62 to 1.506 eV. This is because of the compression of the unit cell, leading to an increase in the charge overlap. In the interval $p = 70$–100 GPa, the band gap decreases suddenly, with a similar change in the C13—N5 bond (see Fig. 7c). The smaller the band gap, the easier the electrons move from the valence band to the conduction band. This means that MT is more sensitive at high pressures.

The density of states is a useful method to analyze pressure-induced changes in the electronic structure. The calculated density of states of MT is shown in Fig. 8b with the Fermi level plotted by the dashed line. Several conclusions can be drawn from Fig. 8. First, the number of peaks becomes smaller as the pressure increases. There are five main peaks at $p = 0$, and only three main peaks are left at $p = 80$–100 GPa. This happens because more and more orbitals become hybridized at high pressure. Second, the top of the valence band and the bottom of the conduction band are mainly composed of p orbitals, indicating that they play an important role in the chemical reaction. Moreover, the conduction band is shifted to a lower energy area with an increase in pressure.

Table 5. Calculated bond orders in the MT cocrystal

Bond	Bond order
Cl1—O1	0.44
Cl2—O7	0.45
Cl3—O10	0.44
Cl4—O15	0.46
Cl5—O20	0.43
Cl6—O21	0.42
N1—C2	0.73
N2—C5	0.74
N3—C9	0.72
N4—C7	0.74
N5—Cl3	0.6
N6—Cl4	0.61

2.6. Bond Order Analysis

The bond order is a measure of the overall bond strength between two atoms, i.e., the larger the bond order, the greater the bonding overlap, leading to bonds that are stronger and more resistant to rupture. The calculated natural bond orders of MT are listed in Table 5. The orders of Cl—O bonds (such as Cl1—O1, Cl2—O7, Cl3—O10, etc.) are much lower than those of other bonds, indicating that the Cl—O bonds are much weaker and easier to break up.

CONCLUSIONS

In this work, a "one-plot" method was employed to synthesize a new kind of a cocrystal energetic material: methylamine triethylenediamine triperchlorate. The performance tests of MT show that the sensitivity of MT is much lower than that of PETN, but a little

higher than that of TNT. The detonation performance of MT is much better than that of TNT. The investigations of the crystal structure show that there is a new typical kind of trigeminal-type hydrogen bonds in the structure: the hydrogen atom from amine can form three hydrogen bonds with the oxygen atom from three different perchlorates, which can form strong inter- and intramolecular hydrogen bonds to stabilize the cocrystal. The band structure analysis of MT shows that the top of the valence bands has large dispersion, whereas the bottom of the conduction bands has rather small dispersion. It is demonstrated that the lattice parameters and the unit cell volume are affected by pressure. At high pressures, the hydrogen bonds become shorter, while the density increases, which can enhance the detonation performance. The density of state analysis of MT at high pressures indicates that *p*-orbitals plays an important role in the chemical reaction. The bond order analysis shows that the Cl—O bond is much weaker than other bonds.[3]

The work was supported by the China Postdoctoral Science Foundation (Grant No.2014M551579) and by the Priority Academic Program Development of Jangsu Higher Education Institutions and Postdoctoral of Jiangsu Province (Grant No. 1401104C).

REFERENCES

1. D. Badgujar, M. Talawar, S. Asthana, and P. Mahulikar, "Advances in Science and Technology of Modern Energetic Materials: an Overview," J. Hazard. Mater. **151** (2), 289–305 (2008).
2. B. M. Rice, J. J. Hare, and E. F. C. Byrd, "Accurate Predictions of Crystal Densities Using Quantum Mechanical Molecular Volumes," J. Phys. Chem. A **111** (42), 10874–10879 (2007).
3. A. A. Dippold, D. Izsak, and T. M. Klapotke, "A Study of 5-(1,2,4-triazol-c-yl)tetrazol-1-ols: Combining the Benefits of Different Heterocycles for the Design of Energetic Materials," Chem.-Eur. J. **19** (36), 12042–12051 (2013).
4. H. Xue, Y. Gao, B. Twamley, and J. M. Shreeve, "Energetic Azolium Azolate Salts," Inorg. Chem. **44** (14), 5068–5072 (2005).
5. P. Yin, D. A. Parrish, and J. M. Shreeve, "Energetic Multifunctionalized Nitraminopyrazoles and Their Ionic Derivatives: Ternary Hydrogen-Bond Induced High Energy Density Materials," J. Amer. Chem. Soc. **137** (14), 4778–4786 (2015).
6. V. D. Ghule, "Computational Screening of Nitrogen-Rich Energetic Salts Based on Substituted Triazinem" J. Phys. Chem. C **117** (33), 16840–16849 (2013).
7. J. Zhang and J. M. Shreeve, "3,3′-Dinitroamino-4,4′-azoxyfurazan and Its Derivatives: An Assembly of Diverse N—O Building Blocks for High-Performance Energetic Materials," J. Amer. Chem. Soc. **136** (11), 4437–4445 (2014).
8. A. E. van der Heijden, R. H. Bouma, and A. C. van der Steen, "Physicochemical Parameters of Nitramines Influencing Shock Sensitivity," Propell., Explos., Pyrotech. **29** (5), 304–313 (2004).
9. A. K. Sikder and N. Sikder, "A Review of Advanced High Performance, Insensitive and Thermally Stable Energetic Materials Emerging for Military and Space Spplications," J. Hazard. Mater. **112** (2), 1–15 (2004).
10. H. Lin, S. G. Zhu, L. Zhang, et al., "Intermolecular Interactions, Thermodynamic Properties, Crystal Structure, and Detonation Performance of HMX/NTO Cocrystal Explosive," Int. J. Quantum Chem. **113** (10), 1591–1599 (2013).
11. C. Guo, H. Zhang, X. Wang, et al., "Crystal Structure and Explosive Performance of a New CL-20/Caprolactam Cocrystal," J. Mol. Struct. **1048** (24), 267–273 (2013).
12. J. P. Shen, X. H. Duan, Q. P. Luo, et al., "Preparation and Characterization of a Novel Cocrystal Explosive," Cryst. Growth Des. **11** (5), 1759–1765 (2011).
13. J. F. Remenar, S. L. Morissette, M. L. Peterson, et al., "Crystal Engineering of Novel Cocrystals of a Triazole Drug with 1,4-Dicarboxylic Acids," J. Amer. Chem. Soc. **125** (28), 8456–8457 (2003).
14. D. R. Weyna, T. Shattock, P. Vishweshwar, and M. J. Zaworotko, "Synthesis and Structural Characterization of Cocrystals and Pharmaceutical Cocrystals: Mechanochemistry vs Slow Evaporation from Solution," Cryst. Growth Des. **9** (2), 1106–1123 (2009).
15. C. Y. Zhang, Z. W. Yang, X. Q. Zhou, et al., "Evident Hydrogen Bonded Chains Building CL-20-Based Cocrystals," Cryst. Growth Des. **14** (8), 3923–3928 (2014).
16. D. Millar, H. Maynard-Casely, D. Allan, et al., "Crystal Engineering of Energetic Materials: Co-Crystals of CL-20," Crystengcomm. **14** (10), 3742–3749 (2012).
17. K. B. Landenberger and A. J. Matzger, "Cocrystal Engineering of a Prototype Energetic Material: Supramolecular Chemistry of 2,4,6-trinitrotoluene," Cryst. Growth Des. **10** (12), 5341–5347 (2010).
18. O. Bolton and A. J. Matzger, "Improved Stability and Smart-Material Functionality Realized in an Energetic Cocrystal," Angew. Chem. Int. Edit. **50** (38), 8960–8963 (2011).

[3]Supplementary data CCDC1435060 contain supplementary crystallographic data for MT. These data can be obtained free of charge via http://www.ccdc.cam.ac.uk/conts/retrieving.html, or from the Cambridge Crystallographic Data Centre, 12 Union Road, Cambridge CB2 1EZ, UK; fax: +44 1223 336 033; or e-mail: deposit@ccdc.cam.ac.uk.

19. K. B. Landenberger and A. J. Matzger, "Cocrystals of 13,5,7-tetranitro-1,3,5,7-tetrazacyclooctane (HMX)," Cryst. Growth Des. **12** (7), 3603–3609 (2012).
20. O. Bolton, L. R. Simke, P. F. Pagoria, and A. J. Matzger, "High Power Explosive Withgood Sensitivity: A 2:1 Cocrystal of CL-20: HMX," Cryst. Growth Des. **12** (9), 4311–4314 (2012).
21. H. Lin, Sh.-G. Zhu, and L. Zhang, "Theoretical Investigation of a Novel High Density Cage Compound 4,8,11,14,15-pentanitro-2,6,9,13-tetraoxa-4,8,11,14,15-pentaazaheptacyclo[5.5.1.13,11.15,9] pentadecane," J. Mol. Model. **19** (3), 1019–1026 (2013).
22. H. Lin, Sh.-G. Zhu, and H.-Zh. Li, "Synthesis, Characterization, AIM and NBO Analysis of HMX/DMI Cocrystal Explosive," J. Mol. Struct. **1048** (24), 339–348 (2013).
23. H. Lin, P.-Y. Chen, and Sh. Zhu, "Computational Study of Pyrazine-Based Derivatives and TheirN-Oxides As High Energy Materials," J. Phys. Org. Chem. **16** (6), 484–491 (2013).
24. H. Lin, P.-Y. Chen, Sh.-G. Zhu, et al., "Theoretical Studies on the Thermodynamic Properties, Densities, Detonation Properties, and Pyrolysis Mechanisms of Trinitromethyl-Substituted Aminotetrazole Compounds," J. Mol. Model. **19** (6), 2413–2422 (2013).
25. D. Guo, Q. An, S. V. Zybin, et al., "The Co-Crystal of TNT/CL-20 Leads to Decreased Sensitivity Toward Thermal Decomposition from First Principles Based Reactive Molecular Dynamics," J. Mater. Chem. A. **3** (10), 5409–5419 (2015).
26. P. Ma, L. Zhang, Sh. Zhu, and H. Chen, "Synthesis, Crystal Structure and DFT Calculation of an Energetic Perchlorate Amine Salt," J. Cryst. Growth. **335** (1), 70–74 (2011).
27. P. Ma, L. Zhang, Sh.-G. Zhu, and H.-H. Chen, "Synthesis, Structural Investigaqtion, Thermal Destruction, and Properties of a Cocrystal Energetic Perchlorate Amine Salt," Fiz. Goreniya Vzryva **48** (4), 123–128 (2012) [Combust., Expl., Shock Waves **48** (4), 483–487 (2012)].
28. G. M. Sheldrick, *SHELXL-97. Program for the Refining of Crystal Structure* (Univ. of Göttingen, 1997).
29. M. D. Segall, P. J. D. Lindan, and M. J. Probert, "First-Principles Simulation: Ideas, Illustrations and the CASTEP Code," J. Phys. **14** (11), 2717–2744 (2002).
30. T. H. Fischer and J. Almlof, "General Methods for Geometry and Wave Function Optimization," J. Phys. Chem. **96** (24), 9768–9774 (1992).
31. M. Anniyappan, S. H. Sonawane, S. J. Pawar, and A. K. Sikder, "Thermal Decomposition and Kinetics of 2,4-dinitroimidazole: An Insensitive High Explosive," Thermochim. Acta **614**, 93–99 (2015).
32. W. H. Zhu, J. J. Xiao, G. F. Ji, F. Zhao, and H. M.Xiao, "First-Principles Study of the Four Polymorphs of Crystalline Octahydro-1,3,5,7-tetranitro-1,3,5,7-tetrazocine," J. Phys. Chem. B **111** (44), 12715–12722 (2007).
33. M. M. Kuklja, E. V. Stefanovich, and A. B. Kunz, "An Excitonic Mechanism of Detonation Initiation in Explosives," J. Chem. Phys. **112** (7), 3417–3423 (2000).
34. G. J. Gilman, "Fast, Faster, and Fastest Cracks," Phil. Mag. Lett. **77** (2), 79–82 (1998).
35. Q. Wu, W. H. Zhu, and H. M. Xiao, "Pressure-Induced Hydrogen Transfer and Polymerization in Crystalline Furoxan," RSC Adv. **4** (31), 15995–16004 (2014).
36. Q. Wu, W. H. Zhu, and H. M. Xiao, "Structural Transformations and Absorption Properties of Crystalline 7-amino-6-nitrobenzodifuroxan under High Pressures," J. Phys. Chem. C **117** (33), 16830–16839 (2013).
37. W. Zhu and H. Xiao, "First-Principles Band Gap Criterion for Impact Sensitivity of Energetic Crystals: A Review," Struct. Chem. **21** (3), 657–665 (2010).